ZraP, the most prominent zinc protein under zinc stress conditions has no direct role in in-vivo zinc tolerance in Escherichia coli

van der Weel, Laura; As, Karel S.; Dekker, Wijb J.C.; van den Eijnden, Lieke; van Helmond, Ward; Schiphorst, Christo; Hagen, Wilfred R.; Hagedoorn, Peter Leon

DOI
10.1016/j.jinorgbio.2018.12.013

Publication date
2019

Document Version
Final published version

Published in
Journal of Inorganic Biochemistry

Journal of Inorganic Biochemistry 192 (2019) 98–106

Contents lists available at ScienceDirect

Journal of Inorganic Biochemistry

journal homepage: www.elsevier.com/locate/jinorgbio

ZraP, the most prominent zinc protein under zinc stress conditions has no direct role in *in-vivo* zinc tolerance in *Escherichia coli*

Laura van der Weel, Karel S. As, Wijb J.C. Dekker, Lieke van den Eijnden, Ward van Helmond, Christo Schiphorst, Wilfred R. Hagen, Peter-Leon Hagedoorn*

Department of Biotechnology, Delft University of Technology, Van der Maasweg 9, 2629 HZ Delft, the Netherlands

ARTICLE INFO

Keywords:
ZraP
Zinc tolerance
Isothermal Titration Calorimetry
Escherichia coli

ABSTRACT

Escherichia coli ZraP (zinc resistance associated protein) is the major Zn containing soluble protein under Zn stress conditions. ZraP is the accessory protein of a bacterial two-component, Zn^{2+} sensitive signal transduction system ZraSR. ZraP has also been reported to act as a Zn^{2+} dependent molecular chaperone. An explanation why ZraP is the major Zn protein under the stress condition of Zn^{2+} overload (0.2 mM) has remained elusive. We have recombinantly produced *E. coli* ZraP and measured Zn^{2+} and Cu^{2+} affinity *in-vitro* using Isothermal Titration Calorimetry. ZraP has a significantly higher affinity for Cu^{2+} than for Zn^{2+}. Mutation of the conserved Cys^{102} to Ala or Ser resulted in a change of the oligomeric state of the protein. Mutation of the conserved His^{107} to Ala did not affect the zinc binding affinity or the oligomeric state of the protein. Deletion of the ZraP coding gene from the *E. coli* genome resulted in a phenotype with tolerance to very high zinc concentrations (up to 2.5 mM) that were lethal to wild type *E. coli*. These results exclude a direct role for ZraP in Zn^{2+} tolerance in *E. coli*.

1. Introduction

Zinc is an essential trace element in all forms of life and zinc containing proteins and enzymes are ubiquitous in nature. Important biochemical functions of zinc in enzymes are: to act as a Lewis acid catalyst (*e.g.* in carbonic anhydrase), or as a structural component in DNA binding zinc finger proteins. Zinc concentrations above 0.2 mM are toxic to *Escherichia coli*, which exemplifies the necessity for zinc homeostasis in this organism. In *E. coli* Zn^{2+} is present in micromolar concentrations in the cytoplasm, but free Zn^{2+} is essentially absent (femtomolar range) [1]. Genomic and proteomic investigations of zinc homeostasis in *E. coli* showed an important role of the periplasmic efflux pump ZnuABC, an ATP Binding Cassette transporter for Zn^{2+} transport from the cytoplasm to the periplasm. Genomic investigation of *E. coli* cultivated in the presence 0.2 mM Zn^{2+}, a zinc stress condition, identified ZraP (zinc resistance associated protein) as the protein that was most upregulated (47 fold increase) compared to the absence of added zinc [2]. However a proteomic study, based on 2D-PAGE and MS protein identification, under similar conditions did not show ZraP at all [3]. This observation is at odds with the fact that ZraP was discovered as a protein overexpressed under high zinc levels [4].The lack of ZraP in the proteomics data was attributed to the pI of 9.1 for this protein which was too high for the 2D-PAGE.

ZraP was originally discovered as a 12 kDa protein called YjaI and induced by a Zn^{2+} dependent transcriptional regulator PMTR (*Proteus mirabilis* transcriptional regulator) that was heterologously expressed in *E. coli* in the presence of Zn^{2+} [4]. A function in zinc homeostasis for ZraP was proposed, but its physiological role remained enigmatic. More than ten years after the original discovery we found in a MIRAGE (Metal Isotope native RadioAutography in Gel Electrophoresis) metalloproteomics study that ZraP was the main zinc containing protein in *E. coli* under zinc stress conditions [5]. This was evidence that ZraP is a zinc containing protein *in-vivo*, consistent with the fact that the protein was already identified to be able to bind zinc [4]. In an independent study *Salmonella typhimurium* ZraP was found to acts as a repressor of the transcriptional regulatory system ZraSR (previously named HydGH) and appeared to function as a zinc dependent molecular chaperone [6,7]. More recently ZraP was biochemically characterized in more detail [8]. *E. coli* ZraP was found to be an octamer with four Zn^{2+} binding sites. The Zinc binding sites presumably contribute to the dimerization of ZraP monomers, a C-terminal domain contributes to the further oligomerization of the dimers to the octameric structure.

The only structural information on ZraP is from an unpublished structure of *Salmonella enterica* ZraP that has been deposited in the

* Corresponding author.
E-mail address: p.l.hagedoorn@tudelft.nl (P.-L. Hagedoorn).

https://doi.org/10.1016/j.jinorgbio.2018.12.013
Received 1 October 2018; Received in revised form 28 November 2018; Accepted 21 December 2018
Available online 27 December 2018
0162-0134/

protein databank (3LAY.pdb). This structure shows ZraP as a homo-decameric ring shaped oligomer. Despite the fact that the reported crystallization conditions include 0.2 mM zinc acetate, no Zn atoms were found in the structure. The part of the protein that includes putative metal binding amino acid residues was not resolved in the structure.

ZraP has been implicated as a gene upregulated when *E. coli* is subjected to heavy metals [9]. A 2.1 fold upregulation of ZraP was found after exposure to a mixture of heavy metals, which included 0.3 mM Zn^{2+}. No upregulation of ZraP expression was found in response to metals other than zinc. The response of the ZraSR system to Pb^{2+}, with concomitant overexpression of ZraP, has been shown by others [10]. Based on this finding a ZraSRP based fluorescent sensing and removal system was developed for Zn^{2+} and Pb^{2+} [11,12]. In this system only the promotor region of ZraP was used to control the expression of GFP (green fluorescent protein) and OmpC (outer membrane protein C), a Pb^{2+} binding peptide. ZraSR induces activation of the ZraP promoter in a Zn^{2+} dependent manner. The cross-reactivity of the ZraSR system with Pb^{2+} was exploited to visualize lead pollution and to induce bioaccumulation of lead in *E. coli*.

Here we present the direct measurement of Zn^{2+} and Cu^{2+} binding to ZraP with Isothermal Titration Calorimetry. Furthermore, we show that disruption of the *zraP* gene does not decrease the tolerance of *E. coli* for Zn. In fact the ZraP disruption mutant exhibited a higher tolerance to zinc concentrations above 0.5 mM. Implications for the physiological role of this protein are discussed.

2. Materials and methods

2.1. Expression of ZraP

Detailed information about the strains and plasmids that have been used are given in Table 1. *E. coli* BL21 genomic DNA was isolated using the GenElute Bacterial Genomic DNA kit. The *zraP* coding gene, excluding the leader sequence, residue 1–26 (Fig. 1), was amplified using PCR (Biometra) with the following primers: ZraP-F 5′-GCCATGGCATG AAACGGAACACG-3′; ZraP-R 5′-AAAGAATCTTTACCAGTGGCCC ATA-3′. The forward primer included an *Nco*I restriction site (underlined). No restriction site was included in the reverse primer, but the *Eco*RI restriction site of the pCR2.1 TOPO-TA subcloning vector was used for cloning. This resulted in the incorporation of 6 additional basepairs downstream of the *zraP* gene originating from the TOPO vector (pCR2.1-TOPO). PCR was performed with Pfx polymerase (Invitrogen) and an annealing temperature of 55 °C was used. The resulting PCR product was subcloned using TOPO TA cloning (Invitrogen). The resulting TOPO vector containing the *zraP* gene was sequenced using M13 primers by the company Baseclear (Leiden, The Netherlands). The sequence matched 100% with the *zraP* gene (NCBI Reference sequence NC_012892.2, excluding the leader sequence). The pCR2.1 TOPO-zraP and pBAD plasmids (Invitrogen) were digested using *Nco*I and *Eco*RI (New England Biolabs) and the proper fragments were isolated using the Qiagen gel isolation kit. Ligation was performed using T4 ligase (Promega). The ligation was performed at room temperature for 1 h with a molar ratio of pBAD vector and *zraP* insert of 1:10. *E. coli* TOP10 (Invitrogen) was transformed using the resulting ligated vector. *E. coli* TOP10 containing pBAD-ZraP was cultivated on LB medium at 37 °C until and OD600 = 0.8. ZraP expression was induced by addition of 0.02% (w/v) arabinose (Sigma-Aldrich) and cells were harvested after 4 h at 37 °C. Cells were harvested by centrifugation at 20,000*g* for 1 h at 4 °C using a Sorvall centrifuge (Thermo). The cell pellet was washed using 50 mM Tris pH 9.0 and subsequently resuspended in the same buffer. Cells were broken using a Cell disruptor at 1.5 kbar (Constant Systems). Cell-free extract (CFE) was obtained as the supernatant after centrifugation at 20,000*g* for 1 h at 4 °C. SDS-PAGE was performed using 10% Criterion XT precast gels (Bio-Rad). Native PAGE of purified ZraP was performed using 4–15% PhastGel and the PhastSystem (GE Healthcare). SDS-PAGE with reducing and non-reducing conditions was performed using a 12% Criterion XT Bis-Tris protein gel (Bio-Rad). XT sample buffer and XT reducing agent was used. XT reducing agent is a pH neutral and stabilized TCEP solution. The reducing agent was omitted for the samples without reducing conditions. The samples were heated for 5 min at 95 °C. 30 µl sample containing 10, 20 or 40 µg protein was loaded per well. Precision Plus Protein standard (Bio-Rad) was used as the marker. The gel was run for 45 min at 200 V.

2.2. Disruption of the zraP gene from the E. coli genome

Markerless deletion of the zraP gene was performed using the pRed/ET recombination procedure using protocols recommended by the manufacturer (Gene Bridges). The FRT-Kan cassette with homology to the *zraP* gene was constructed by PCR using the following primers: forward primer 5′-GGCACGGAAGATGCAATACCCGAAGTAAGACA ACCACTGGAGGATTAACCAATTAACCCTCACTAAAGGGCG-3′; reverse primer 5′-GGCAAACTCTGATTTCTGTCGCTGGCAACCCAACGAGAAAA CGTTCTGATTAATACGACTCACTATAGGGCTC-3′ and the FRT-PGK-gb2-neoFRT template. The underlined sequences are homologous to the FRT cassette, the rest to the *zraP* gene. FRT is a Flippase recognition target site. Chemically competent *E. coli* TOP10 cells were transformed with the pRedET-amp vector. Transformants were selected on LB-agar containing 50 µg/ml ampicillin. pRedET-amp contains the λ phage operon *redγβα* under the control of an arabinose inducible promotor. The cells were cultivated in LB medium for 2 h at 30 °C and subsequently 0.4% L-arabinose was added to induce the recombination proteins Redα, Redβ and Redγ. Shortly thereafter chemically competent cells were prepared from these cells. These cells were subsequently

Table 1
Bacterial strains and plasmid used in this work.

	Phenotype or characteristics	Source or reference
Strains		
E. coli TOP10	*mcrA, Δ(mrr-hsdRMS-mcrBC), φ80lacZ(del)M15, ΔlacX74, deoR, recA1, araD139, Δ(ara-leu)7697, galU, galK, rpsL(SmR), endA1, nupG*	Invitrogen
E. coli BL21	*fhuA2 lon ompT gal dcm ΔhsdS*	New England Biolabs
E. coli TOP10 *ΔzraP*	Markerless deletion *zraP* gene	This work
Plasmids		
pCR2.1-TOPO TA	Subcloning vector, 3′-T overhang, Topoisomerase I covalently bound	Invitrogen
pBAD/His	Expression vector, ara promotor, Amp resistance marker	Invitrogen
pBAD-ZraP	Expression *E. coli* BL21 ZraP excluding leader sequence	This work
pBAD-ZraP^{C102A}	Expression *E. coli* BL21 ZraP^{C102A} excluding leader sequence	This work
pBAD-ZraP^{C102S}	Expression *E. coli* BL21 ZraP^{C102S} excluding leader sequence	This work
pBAD-ZraP^{H107A}	Expression *E. coli* BL21 ZraP^{H107A} excluding leader sequence	This work
pRED/ET-amp	Expression recombination proteins Redγβλ, Amp resistance	Gene Bridges
pCP20	Flippase expression, Amp resistance	Gene Bridges

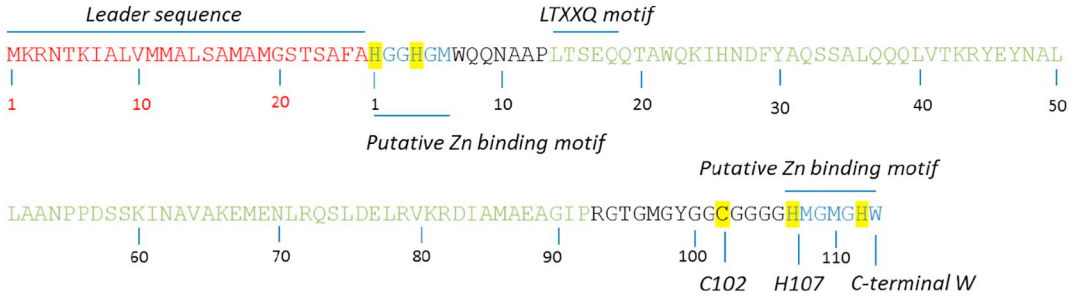

Fig. 1. ZraP amino acid sequence. In red the leader sequence for periplasmic localization, as experimentally confirmed to be cleaved *in-vivo* [4]. In blue are putative Zn^{2+} binding motifs that have been proposed previously [4]. Putative Zn^{2+} coordinating amino acids are highlighted in yellow. In green the AA sequence that is in the known crystal structure. Note that all putative Zn^{2+} binding ligands are outside this sequence. No Zn^{2+} was detected in the crystal structure. The calculated molecular mass excluding leader sequence is 11.9 kDa, and 15.0 kDa including leader sequence. The calculated pI of the protein excluding leader sequence is 6.82 and 9.17 with leader sequence.

transformed with the FRT-Kan cassette containing the *zraP* gene homology arms. The correct integration of the FRT-Kan cassette was confirmed by single colony PCR using the following primers: F_control_zraP 5′-GACAACCACTGGAGGATTAACC-3′; R_control_zraP 5′-CCAACGAGAAAACGTTCTGAT3′. The primers are complementary to the zraP homology arms of the FRT-Kan cassette. Correct integration of the cassette should result in a PCR product of 1737 bp. If the zraP gene is still present a fragment of 421 bp would be amplified. The resulting *E. coli* TOP10 ΔzraP::FRT-Kan was cured from the pRED-amp plasmid by cultivating at 42 °C with three subsequent serial dilutions of 150×. Kanamycin resistant colonies that were sensitive to ampicillin were selected. The Kanamycin resistance marker was removed using the protein flippase that can remove the FRT flanked region. Chemically competent *E. coli* TOP10 *ΔzraP::FRT-Kan* was transformed using the flippase expression plasmid pCP20-amp. Ampicillin resistant colonies were selected. The pCP20-amp containing cells were cultivated overnight at 37 °C in the absence of antibiotics to induce the flippase recombination. PCR using the F_control_zraP and R_control_zraP primers was used to confirm removal of the FRT-Kan cassette. Subsequently the *E. coli* TOP10 *ΔzraP* was cured of the pCP20 plasmid by overnight cultivation on LB in the absence of antibiotics. Ampicillin sensitive colonies were selected and single colony PCR was used to confirm the zraP deletion. Further confirmation of the zraP deletion was obtained by DNA sequencing (Baseclear, Leiden, The Netherlands). The absence of ZraP expression in the zraP deletion mutant was confirmed by performing by SDS-PAGE of *E. coli* TOP10 and *E. coli* TOP10 *ΔzraP* cultivated in the absence and presence of 1 mM $ZnCl_2$. The 12 kDa band of ZraP induced by Zn^{2+}, was absent in the *ΔzraP* cultivated under the same conditions (Fig. S1).

2.3. Mutagenesis

The genes encoding the $ZraP^{C102A}$, $ZraP^{C102S}$ and $ZraP^{H107A}$ mutants were synthesized by the company DNA 2.0 (ATUM, Newark CA, USA). The genes were excised from of the pJ102 vector using *Nco*I and *Eco*RI digestion and ligated into pBAD/B using T4 DNA ligase (New England Biolabs), which was subsequently used to transform chemically competent *E. coli* TOP10 *ΔzraP*. Positive transformants were selected using Ampicillin resistance and the presence of the *zraP* gene was confirmed using colony PCR using the following pBAD primers: pBAD F57 5′-CTCTTCTCGCTAACCAAACC-3′ and pBAD R733 5′- GATTTAATCTG TATCAGG-3′.

2.4. Protein purification

ZraP, $ZraP^{C102A}$, $ZraP^{C102S}$ and $ZraP^{H107A}$ were purified in three chromatographic steps using a Shimadzu HPLC system. 50 ml CFE containing 4 mg/ml protein was filtered using a syringe filter with a 0.45 µm cut-off (Merck) and loaded on a 10 ml DEAE sepharose column (GE Healthcare), equilibrated with 50 mM Tris pH 9.0. A flow rate of 3 ml/min was applied. The column was washed with 5 column volumes (CV) of 50 mM Tris pH 9.0. A linear gradient of 20 CV was applied from 0 to 0.5 M NaCl in 50 mM Tris pH 9.0. ZraP and $ZraP^{H107A}$ eluted between 0.18 and 0.29 M NaCl. $ZraP^{C102A}$ and $ZraP^{C102S}$ did not bind to the column and were collected in the flow through. ZraP elution was identified using SDS-PAGE. Buffer exchange to 50 mM Tris pH 8 was performed using repeating concentration and dilution steps using ultrafiltration (Merck) with a 10 kDa MWCO filter. The ZraP containing sample was applied to a 9 ml Q-sepharose column (GE Healthcare) equilibrated with 50 mM Tris pH 8. A flow rate of 5 ml/min was applied and the column was washed with 5 CV of 50 mM Tris pH 8.0 after loading the protein sample. A gradient of 10 CV from 0 to 0.5 M NaCl in 50 mM Tris pH 8.0 was applied. ZraP and $ZraP^{H107A}$ eluted from 100 to 140 mM NaCl. $ZraP^{C102S}$ and ZraP C^{102A} eluted from 0 to 50 mM NaCl. Buffer exchange to 50 mM HEPES pH 8 containing 150 mM NaCl was performed using repeating concentration and dilution steps using ultrafiltration (Merck) with a 10 kDa MWCO filter. The concentrated sample was injected onto a Superdex S200 column equilibrated with 50 mM HEPES pH 8.0 containing 150 mM NaCl. ZraP elution was determined using SDS-PAGE. The identity of the purified protein was confirmed to be *E. coli* ZraP using protein mass spectrometry as described previously [5].

2.5. Metal ion binding to ZraP measured with Isothermal Titration Calorimetry

ITC measurements were performed at 25 °C using a Microcal VP-ITC (Malvern). All solutions were degassed prior to use. Each ITC experiment consisted of 5–15 µl injections of 1 mM $ZnCl_2$ in 150 mM NaCl and 50 mM HEPES pH 7, or 1 mM $CuSO_4$ in 150 mM NaCl and 50 mM Tris pH 7 to 60–70 µM ZraP and $ZraP^{H107A}$ in the identical buffer as the metal ion solution. Tris was chosen as a buffer because solubility of $CuCl_2$ in the HEPES buffer was insufficient, possibly due to $Cu(OH)_2$ precipitation because HEPES does not coordinate Cu^{2+} sufficiently [13]. Control titrations of the Zn and Cu solutions to the buffer without protein under identical conditions were subtracted from the titration with ZraP. Raw data of all measurements including the control measurements can be found in Supplementary Fig. S6.

2.6. Analysis of ZraP sequence

The amino acid sequence of *E. coli* BL21 ZraP was compared to other *E. coli* ZraP sequences using the multiple sequence alignment tools Clustal Omega and ClustalW [14,15]. The resulting alignment is given in Fig. S2. BLAST of BL21 ZraP sequence against non-redundant database excluding *E. coli* resulted in the multiple sequence alignment in Fig. S3. BLAST of BL21 ZraP sequence against non-redundant database excluding Enterobacteria resulted in the multiple sequence alignment given in Fig. S4.

2.7. Effect of Zn^{2+} on the cultivation of E. coli TOP10 and E. coli TOP10 ΔzraP

20 ml of LB medium with 0, 0.2, 0.5 or 1.0 mM $ZnCl_2$ was inoculated with 0.2 ml overnight grown preculture of *E. coli* TOP10 and *E. coli* TOP10 *ΔzraP* and cultivated in a shaking incubator at 37 °C. The optical density at 600 nm (OD_{600}) was measured every hour for 10 h. Above 4 mM $ZnCl_2$ no growth was observed for both strains. The maximum specific growth rate μ_{max} and maximal OD_{600} was determined by fitting the data to the logistic model: $OD_{600} = \frac{OD_{600,max}}{(1 + e^{-\mu_{max} \cdot (t - t_i)})}$ [16]. t_i represents the time at the inflection point of the sigmoidal growth curve. Doubling time in hours was determined as $t_d = \frac{\ln(2)}{\mu_{max}}$.

3. Results and discussion

3.1. High amino acid sequence variation in ZraP among enterobacteria

During the preparation of the recombinant expression of ZraP we noticed small differences in the amino-acid sequence between strains *E. coli* BL21 and TOP10, which are common expression hosts. Multiple sequence alignment of *E. coli* ZraP sequences from the GenBank database showed a variation involving GM repeats in the N-terminal region of the protein (Figs. 1 and S2). Among Enterobacteria the sequence identity is approximately 60%, which shows that there is considerable amino acid variability already within closely related species (Fig. S3).

ZraP is a member of the CpxP family of accessory proteins to two component signal transduction systems ZraSR and CpxAR respectively. CpxP is a periplasmic protein, which interacts with the sensor kinase CpxA to inhibit envelope stress response in the absence of protein misfolding [17]. CpxP has also been reported to facilitate DegP protease/chaperone mediated proteolytic degradation of misfolded proteins. CpxP contains two conserved LTxxQ motifs, while ZraP contains only one. The crystal structure of CpxP shows two bound Zn^{2+} ions, although the Zn^{2+} binding amino acid residues were not conserved among CpxP family proteins. The LTxxQ motif is a characteristic for the CpxP superfamily of proteins (Fig. 1).

BLAST of the *E. coli* BL21 ZraP sequence against the non-redundant database excluding *Enterobacteria* revealed that ZraP was also present in a number of other gram-negative bacteria (Fig. S4). The C-terminal W113, H107 and the GM repeats are conserved among these bacteria, although C102 is not strictly conserved among organisms sharing more than 60% sequence identity with *E. coli* ZraP. A number of bacteria, dominated by sulfate reducers, which share 30–50% sequence identity with *E. coli* ZraP predominantly have C102 in the N-terminal part of the sequence, but lack the C-terminal tryptophan.

Surprisingly the BL21 ZraP sequence was identical (100%) to the sequence of the PR protein of *Capsicum annuum* (Bell pepper, sequence ID: AAM95615). This is most likely a misannotation that resulted from a contamination of the genomic sample with *E. coli* BL21.

The fact that the C-terminal tryptophan is conserved among all Enterobacterial ZraP sequences points towards an important functional role of this residue. In light of this, it is interesting that *Saccharomyces cerevisiae* Nar1, a protein involved in cytosolic FeS cluster assembly, has a C-terminal tryptophan, which is conserved among homologous proteins from other Eukaryotes, such as *Homo sapiens* Narf [18,19]. The Semliki Forest viral capsid has a C-terminal tryptophan for which a role in autoproteolytic activity of this protein has been described [20]. It is possible that the ZraP C-terminal tryptophan is involved in the cleavage of the leader peptide *in-vivo*. Or it may be important for recognition of other proteins, or the stabilization of the native oligomeric structure.

3.2. Native oligomeric state of ZraP is dependent on Cys^{102}

We have chosen to express ZraP without leader sequence. In a previous publication ZraP was produced including the leader sequence and a C-terminal His-tag [6]. The N-terminus of mature ZraP was determined previously by N-terminal amino acid sequencing. This unequivocally showed that the leader sequence was removed *in vivo* at position 26 [4]. Furthermore a His-tag would introduce a metal cation affinity site that would complicate the interpretation of the Zn^{2+} binding studies. We therefore chose to express the protein recombinantly excluding the leader sequence and without a sequence tag. The protein was highly expressed and could be isolated in three chromatographic steps. Next to the WT protein three different ZraP mutants were expressed in the *ΔzraP* strain: C102A, C102S and H107A. Size exclusion chromatography showed that WT ZraP and $ZraP^{H107A}$ were presumably octameric with a molecular mass of *circa* 96 kDa and 92 kDa respectively, and that the cysteine mutants have a different oligomeric structure presumably monomeric or dimeric, with an apparent molecular mass of *circa* 16 kDa (Fig. 2A and B). Native PAGE of WT ZraP indicated a molecular mass of *circa* 100 kDa, consistent with an octameric structure (Supplementary Fig. S5). Recently, based on analytical ultracentrifugation data ZraP was reported to be octameric. C102 has recently been proposed to form an intersubunit disulfide bridge based on MS analysis, which has been proposed to be required to stabilize the octameric structure [8]. The cysteine mutants were found to have very different structural and charge properties and could not be purified using the same procedure as the WT protein and H107A mutant. Here we propose that C102A and C102S are monomeric, which is consistent with the role of C102 as part of a disulfide bridge that stabilizes the oligomeric state as has been previously proposed. Substoichiometric iron was found in our preparation of ZraP, which was attributed to a contaminating [2Fe-2S] cluster containing protein, as indicated by the UV–vis spectrum with absorbance bands in the visible range at 320 and 420 nm [21]. This contaminating protein co-eluted with ZraP and $ZraP^{H107A}$ and not with the cysteine mutants, which have a different oligomeric state. In order to validate if ZraP contains an intersubunit disulfide bridge SDS-PAGE was performed under reducing and non-reducing conditions (Fig. 2D). The results clearly show a band for ZraP at 12 kDa in all lanes containing reducing agent. This mass corresponds to the unfolded monomeric protein. In the lanes with samples that were treated without reducing agents an additional band appeared which can be attributed to the dimer of 24 kDa. This suggests that ZraP indeed has a disulfide bridge stabilizing dimer formation. The C102S mutation occurs naturally in *Yersinia pestis* ZraP. Considering our finding and the previous report that this cysteine is important for the oligomeric state, we may conclude that this difference apparently did not alter its biological function, assuming it to be the same in *Y. pestis*. It would be interesting to characterize this mutant and determine its metal ion binding affinity. It has been reported that the C102A mutant of ZraP has a different metal ion binding stoichiometry of *circa* 1 per monomer, rather than 0.5 per monomer for WT ZraP [8]. These stoichiometries were determined colorimetrically using equilibrium binding experiments involving EGTA treatment and gel filtration or dialysis to remove non-bound metal ions. The error values in those data, were not reported, so it is not clear if these differences were significant. Furthermore, these differences in stoichiometry may reflect differences in metal affinity compared to EGTA rather than the binding stoichiometry itself.

ZraP expressed containing a C-terminal His-tag and a leader sequence has been found to have an oligomeric state dependent on the zinc concentration: 6–7 meric in the absence of zinc up to 15 meric in the presence of zinc [6]. The deposited crystal structure of *Salmonella enterica* ZraP, heterologously expressed in *E. coli* as an N-terminal His-tagged and leader sequence containing protein, was found to be decameric, with part of the protein structure unresolved in the electron density map (3LAY.pdb). Here we show that ZraP expressed without a His-tag or a leader sequence, identical to the native periplasmic form of the protein, is most likely octameric, although we cannot fully rule out a decameric structure. The molecular mass determination based on size exclusion chromatography assumes that the protein is globular, if ZraP

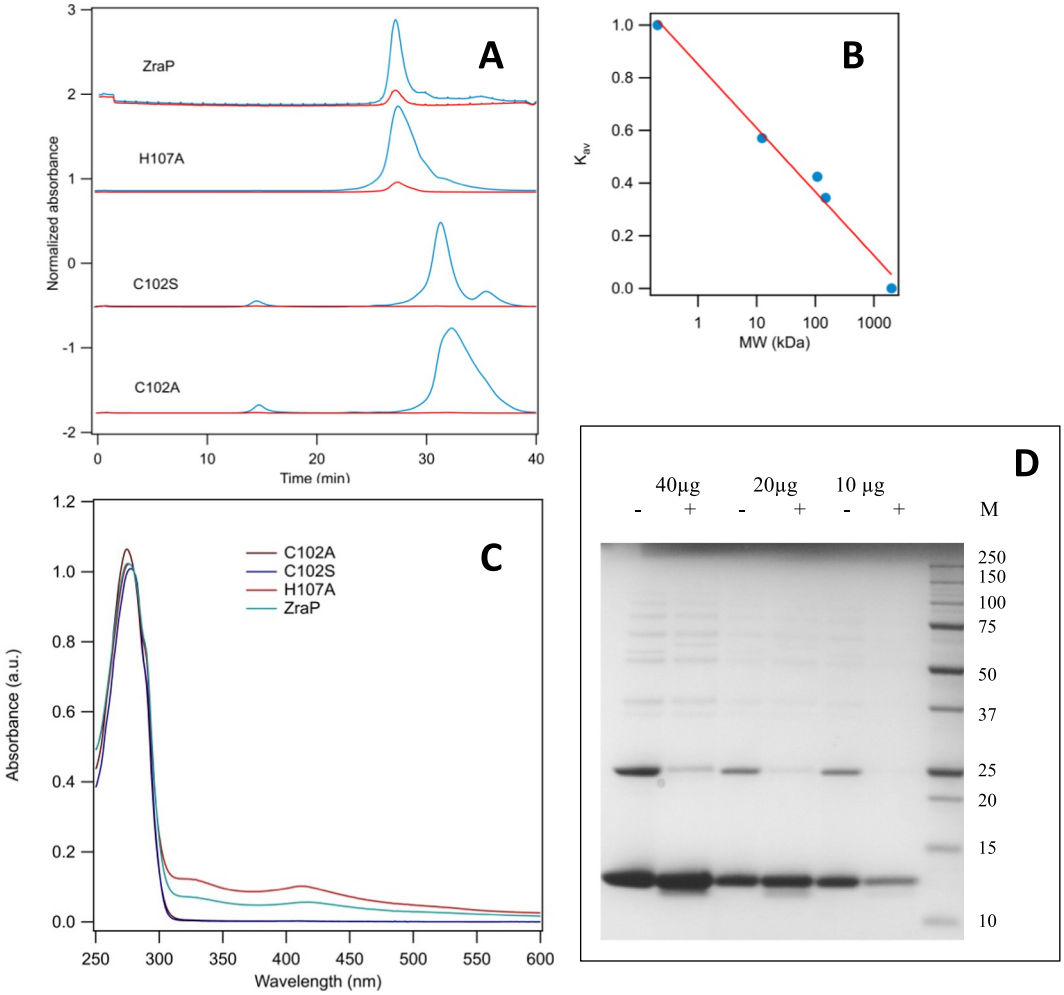

Fig. 2. ZraP oligomeric state determined using size exclusion chromatography. A) chromatograms of ZraP, ZraP^{H107A}, ZraP^{C102S} and ZraP^{C102A}. In red the absorbance at 280 nm, in blue the absorbance at 350 nm. B) Calibration curve of the chromatography column. $K_{AV} = (V_e - V_0)/(V_t - V_0)$ in which V_e is elution volume, V_0 is void volume, and Vt is total volume. Calibration was performed using: blue dextran (2000 kDa), γ-globulin (150 kDa), lipoxidase (108 kDa), cytochrome *c* (12.4 kDa) and tryptophan (0.2 kDa). C) UV–vis spectra of ZraP and mutants from the size exclusion chromatography. All spectra have been normalized to an absorbance at 280 nm of 1.0. D) SDS-PAGE of ZraP denatured with (+) and without (−) reducing agent TCEP. 30 µl sample containing 10, 20 or 40 µg protein was loaded per well. Precision Plus Protein standard (Bio-Rad) was used as the marker.

in solution is a ring shaped multimer (as the structure of *S. enterica* ZraP) the mass determination may be incorrect. Recently, ZraP has been reported to be octameric based on analytical ultracentrifugation [8].

3.3. ZraP has a moderate affinity for Zn^{2+} and a high affinity for Cu^{2+}

ITC was used to measure the binding of Zn^{2+} and Cu^{2+} to ZraP, and Zn^{2+} to ZraP^{H107A}. ZraP was found to bind Zn^{2+} with a K_D of 11.9 ± 0.4 µM and a stoichiometry of 0.55 ± 0.01 Zn^{2+} per monomer (Fig. 3A). Under the conditions used in the ITC experiment the binding reaction was exothermic with a $\Delta H_{ITC} = -61 \pm 1$ kJ/mol. As isolated ZraP was found to contain 0.14–0.24 Zn; 0.01 Cu^{2+} and 0.05–0.06 Fe^{2+} per monomer by HR ICP-MS. The presence of similar sub-stoichiometric amounts of zinc and other metal cations in isolated ZraP has been determined previously [8]. We therefore propose that ZraP can bind one Zn^{2+} ion, and possibly other metal ions as well, per monomer. HEPES buffer has a low affinity for Zn^{2+} with a $K_D = 0.538$ mM at pH 7.4, however the competing effect of the buffer significantly influences the dissociation constant measured with ITC [22]. We can correct for the chelating effect of the HEPES buffer as follows, assuming a 1:1 binding reaction between the metal ion and the buffer:

$$K_a = K_{app} \bullet (1 + K_{a,buffer}[buffer])$$

The buffer-corrected values for the dissociation constant is: $K_D = 126 \pm 4$ nM.

ZraP binds Cu^{2+} with a $K_D = 0.42 \pm 0.05$ µM in Tris buffer and a stoichiometry of 0.50 ± 0.01 per monomer (Fig. 3B). Under the conditions used in the ITC experiment the binding reaction was exothermic with a $\Delta H_{ITC} = -65.7 \pm 0.8$ kJ/mol. Tris buffer was used instead of HEPES as a buffer in the case of Cu to increase the solubility of the metal ion. Tris is a chelating buffer with a high affinity for copper. The apparent affinity of the protein for Cu^{2+} therefore has to be corrected for the competitive binding with Tris [23,24]. Up to two Tris moieties can bind a single Cu^{2+} ion and different ionized forms are known to exist depending on the pH [25].

In this system there are two equilibria in which Cu^{2+} is involved (Scheme 1):

$$K_{app} = \frac{[Cu^{2+} - ZraP]}{[ZraP]([Cu^{2+} - Z] + [Cu^{2+}])}$$

$$K_n = \frac{[CuZ]}{[Cu^{2+}][Tris]}$$

$[CuZ]$ represents the sum of all Cu-Tris complexes. Since the Tris

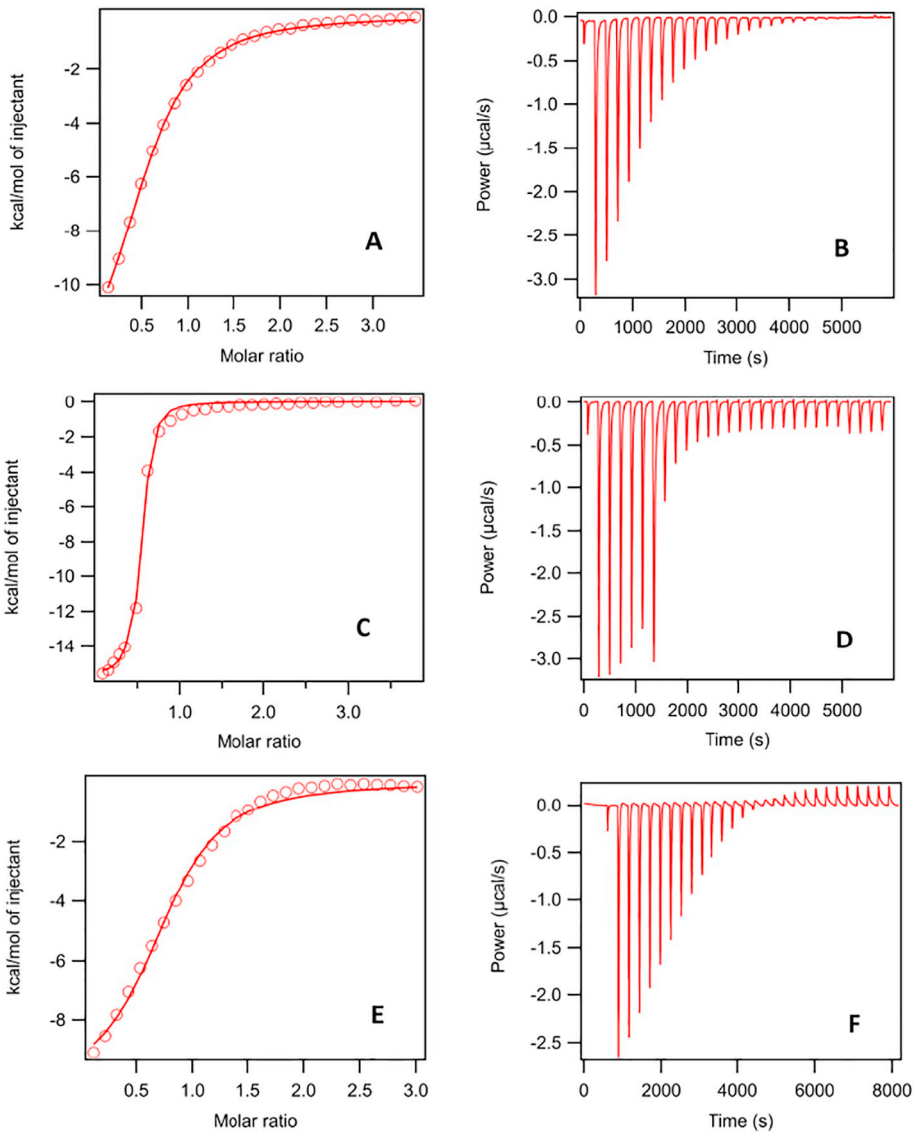

Fig. 3. ITC measurement of the binding of Zn^{2+} and Cu^{2+} to ZraP and the binding of Zn^{2+} to $ZraP^{H107A}$. A and B) Zn^{2+} binding to ZraP. ITC conditions: 64 µM ZraP in 150 mM NaCl, 50 mM HEPES pH 7 in the cell; 1 mM ZnCl2 in 150 mM NaCl, 50 mM HEPES pH 7 in the syringe, all injections 10 µl; Fit parameters: N = 0.55 ± 0.01, $K_{app} = (8.4 \pm 0.3)\cdot 10^4\,M^{-1}$, $\Delta H_{ITC} = -14.6 \pm 0.3$ kcal/mol. C and D) Cu^{2+} binding to ZraP. ITC conditions: 71 µM ZraP in 150 mM NaCl, 50 mM Tris pH 7 in the cell; 1 mM $CuCl_2$ in 150 mM NaCl, 50 mM Tris pH 7 in the syringe, injection 1–5: 5 µl, injection 6–24: 10 µl, injection 25–29: 15 µl; Fit parameters: N = 0.50 ± 0.01, $K_{app} = (2.4 \pm 0.3)\cdot 10^6\,M^{-1}$, $\Delta H_{ITC} = -15.7 \pm 0.2$ kcal/mol. E and F) Zn^{2+} binding to $ZraP^{H107A}$. ITC conditions: 70 µM ZraP in 150 mM NaCl, 50 mM HEPES pH 7 in the cell; 1 mM $ZnCl_2$ in 150 mM NaCl, 50 mM HEPES pH 7 in the syringe. All 10 µl injections; Fit parameters: N = 0.76 ± 0.02, $K_{app} = (1.3 \pm 0.1)\cdot 10^5\,M^{-1}$, $\Delta H_{ITC} = -10 \pm 3$ kcal/mol.

$$Cu^{2+}\text{-}Tris_n + ZraP \underset{Tris}{\overset{K_{app}}{\rightleftharpoons}} Cu^{2+}\text{-}ZraP$$

$$Cu^{2+} + n\ Tris \overset{K_n}{\rightleftharpoons} Cu^{2+}\text{-}Tris_n$$

$$Cu^{2+} + ZraP \overset{K_{real}}{\rightleftharpoons} Cu^{2+}\text{-}ZraP$$

Scheme 1. Binding equilibria of Cu^{2+} to ZraP and Tris buffer.

concentration is in large excess, we assume that the free Tris concentration is equal to the total Tris concentration. The K_n is equal to the competitivity index as reported previously, which represents a conditional affinity constant at a particular pH and total concentration of metal and ligand [26,27]. The Cu-Tris complexes were simulated using Hyperquad simulation program HySS2009 using the affinity and ionization data reported by Nagaj et al. [25,28]. At pH 7 and large excess of Tris over Cu the Cu-Tris speciation is dominated by $CuH_{-1}Tris_2$ (79.4%) and $CuH_{-2}Tris_2$ (11.2%) and $CuH_{-1}Tris$ (6.31%). All other complexes are less than 3.1% (Fig. S7).

The affinity constant for Cu-ZraP is:

$$K_a = \frac{[Cu^{2+} - ZraP]}{[Cu^{2+}][ZraP]}\ K_a = K_{app}\cdot(1 + K_n[Tris])$$

$$= 2.4\cdot 10^6\cdot(1 + 6.03\cdot 10^4\cdot 0.042) = 6.08\cdot 10^9 M^{-1}$$

This would suggest that the affinity of ZraP for Cu^{2+} is very high, with a dissociation constant $K_d = 1.64\cdot 10^{-10}$ M. Binding of Cu^{2+} to BSA has been reported to be in the order of 10^{13} [29]. A more detailed investigation into the effect of a proton release upon binding of Cu^{2+} to ZraP, and the equilibration with the buffer, would be required to establish a definitive K_a for binding of Cu^{2+} to ZraP. It is clear, however, that ZraP has a higher affinity for copper than for zinc by at least two orders of magnitude.

The H107A mutant was found to bind Zn^{2+} with a $K_d = 7.7 \pm 0.5$ µM and a stoichiometry of 0.76 ± 0.02 (Fig. 3C). The dissociation constant corrected for the chelating effect of the HEPES buffer is $K_d = 82 \pm 5$ nM. Under the conditions used in the ITC

experiment the binding reaction was exothermic with a $\Delta H_{ITC} = -42 \pm 12$ kJ/mol. The affinity is similar to the WT protein. The zinc binding stoichiometry was higher for this protein, which may be due to a lower metal content of this protein preparation. This clearly shows that this conserved histidine is not directly involved in the binding of the metal ion or in the stabilization of the oligomeric state (Fig. 2A).

The presence of Zn^{2+} in as isolated ZraP is consistent with the substoichiometric binding of Zn^{2+} in the ITC experiments, *i.e.* the N value is between 0.5 and 0.7. The dissociation constant of ZraP for zinc is consistent with the fact that in the MIRAGE metalloproteomics experiment ZraP was found as a zinc containing protein when the cells were grown in the presence of 0.2 mM Zn^{2+} [5]. However, for a zinc binding protein a K_D of 126 nM is not very high. Furthermore, the fact that the protein can bind other divalent metal cations with similar or even higher affinity may point to a more diverse role of ZraP related to other divalent metal cations. ZraP binds up to one Zn ion per monomer. These properties exclude a role as a zinc storage or buffer protein as was initially proposed by us [5].

3.4. Disruption of *zraP* gene increases *E. coli* tolerance to millimolar zinc levels

Increasing levels of Zn^{2+} in the range 0.2–1.0 mM clearly increased the doubling time and reduced the maximal OD_{600} that was obtained in the growth curves for both WT and *ΔzraP* strains as compared to the growth in the absence of added zinc (Fig. 4A and B). Targeted disruption of the *zraP* gene did not significantly change the growth of *E. coli* TOP10 on LB medium and also did not significantly change the growth of *E. coli* TOP10 on LB medium supplemented with zinc concentrations up to 0.5 mM (Figs. 4A and B and S8). The only zinc related phenotype for the *ΔzraP* mutant was an increased tolerance towards very high Zn^{2+} above 0.5 mM. The μ_{max} was not significantly different between WT and *ΔzraP* strains (Fig. 4A), however, a significantly higher maximal OD_{600} was found for *ΔzraP* than WT *E. coli* above 0.5 mM Zn^{2+} (Figs. 4B and S8). On solid media supplemented with 2.5 mM $ZnCl_2$ *E. coli* TOP10 was not able to grow, but the *ΔzraP* mutant was viable (Fig. 4C and D). Above 4 mM $ZnCl_2$ no growth was observed in liquid cultures and on plate for both strains (not shown). This contradicts with a role of ZraP in Zn^{2+} tolerance, however, it can be consistent with a more subtle regulatory function related to Zn^{2+}. Furthermore, a non-essential role as a Zn^{2+} buffer cannot be excluded. Despite the fact that in *E. coli* ZraP expression is strongly induced under high zinc conditions, and ZraP is clearly a zinc binding protein *in-vitro* and (under zinc stress conditions) *in-vivo*, *E. coli* is more tolerant to high zinc levels without ZraP.

The structure of *S. enterica* ZraP (pdb 3LAY) did not contain any zinc atoms. The crystallization conditions were: 0.2 M sodium chloride, 0.1 M Bis-tris, 25% (w/v) PEG 3350, 0.2 mM Zn acetate, pH 6.5. Although the zinc concentration was reasonably high, we may assume that the protein concentration was even higher. If a 1 mM monomer ZraP concentration was used for crystallization, then every decamer would only contain *circa* 2 Zn^{2+}, which can be bound at different positions in every protein. This may explain why the N-terminal part of the protein, most likely involved in metal binding, was not resolved in the structure. The protein was expressed including an N-terminal his-tag and including the leader sequence, which we know not to be present in the mature native protein. This may have contributed to the difference with the octameric native oligomeric state in solution found by us and others [8].

ZraP has been reported to act as a Zn^{2+} dependent chaperone based on an *in-vitro* thermal stabilization assay of malate dehydrogenase in two separate publications, with identical results [6,8]. In one of these reports ZraP was expressed containing the N-terminal leader sequence, and a C-terminal His-tag [6]. While chaperones are ATP dependent, ZraP was proposed to be zinc dependent, perhaps using Zn^{2+} association and dissociation to induce conformational changes that may assist in protein folding. Direct evidence of a chaperone function *in-vivo* has

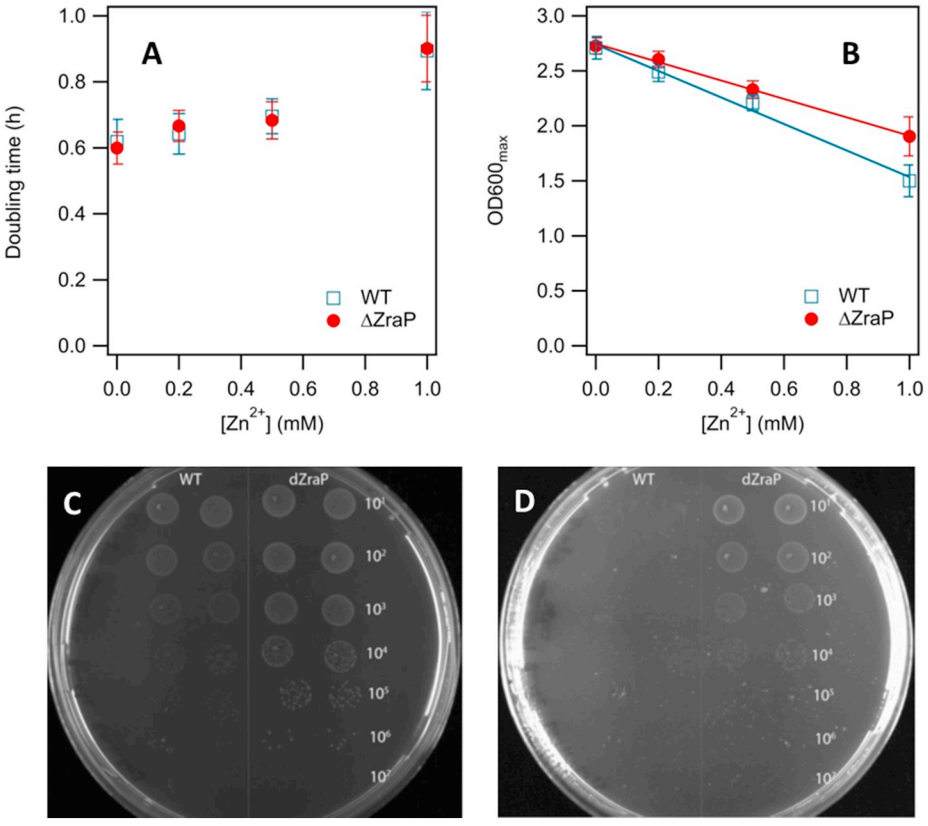

Fig. 4. Effect of high zinc concentrations on the growth of *E. coli* and *E. coli* without ZraP. A) Doubling times of *E. coli* TOP10 and *E. coli* TOP10 *ΔzraP* on liquid LB media at 37 °C supplemented with increasing $ZnCl_2$ concentrations; B) Maximal OD600 determined from the growth curves used to determine the doubling time; C) serial dilution of *E. coli* TOP10 and *E. coli* TOP10 *ΔzraP* on LB-agar containing 2.0 mM $ZnCl_2$; D) serial dilution of *E. coli* TOP10 and *E. coli* TOP10 *ΔzraP* on LB-agar containing 2.5 mM $ZnCl_2$. The precultures were normalized to the same OD600 prior to the serial dilutions and 10 µl of the dilution was spotted on the plate. Plates were incubated 18 h at 37 °C prior to the photograph.

not been established to date. The fact that *E. coli* TOP10 *ΔzraP* is more tolerant to zinc appears to contradict an important chaperone function under these conditions. At 41 °C, a growth condition which requires chaperone activity, the *E. coli* TOP10 *ΔzraP* was found to be more tolerant to zinc than the WT strain (Supplementary Fig. S9).

A *ΔzraP* mutant has been constructed previously in *Salmonella enterica* [6]. No effect on the growth or survival of *S. enterica* in the presence of 1.5 mM $ZnCl_2$ was observed. A statistically significant decrease in polymyxin G resistance was observed, which indicated a functional overlap with other CpxP family proteins.

3.5. The physiological role of ZraP

A regulatory role of ZraP from *E. coli* and *S. enterica* has been proposed [6,8]. ZraSR is a two component signal transduction system co-regulated with an accessory protein ZraP. This is similar to the CpxAR two component signal transduction system with the periplasmic accessory protein CpxP, which shares sequence homology to ZraP. The transcription of ZraP is upregulated by phosphorylated ZraR. ZraS acts as a Zn^{2+} sensor protein for this small signal transduction system. Zn-bound ZraP may act as a transcriptional repressor of zraSR and zraP itself. The precise function of this negative feedback loop is unclear. Based on the *in-vitro* chaperone activity of ZraP and the relationship with CpxP, a role in envelope stress response has been hypothesized [8]. Zinc bound ZraP has been proposed to alleviate envelope stress, in conjunction with the CpxARP system. And the negative feedback loop may act to adapt to sustained activation. This hypothesis, however, does not answer why deletion of the *zraP* gene would make *E. coli* more tolerant to Zn^{2+} above 0.5 mM, and why it is zinc responsive, while the protein has a higher affinity for Cu^{2+}.

The previously reported chaperone activity of ZraP is unfortunately not convincing. This evidence is based on *in-vitro* experiments that showed a protective effect of ZraP on thermal denaturation of malate dehydrogenase (MDH) as monitored by light scattering in two independent studies [6,8]. There are several problems with these reported chaperone activity measurements: 1) MDH was combined with stoichiometric and excess amounts of ZraP, which may have a significant effect on the light scattering; 2) A fourfold difference in light scattering at 360 nm was observed despite similar MDH concentrations and assay conditions, which may be due to different ZraP concentrations; 3) The effect of Zn^{2+} addition on the effect of ZraP was different in each report; 4) in the report by Appia-Ayme et al. *Salmonella enterica* ZraP was expressed including an uncleaved leader peptide and a C-terminal his-tag, and in the report by Petit-Hartlein *E. coli* ZraP was expressed without leader sequence and his-tag.; 5) By a very strange coincidence in both publications the MDH concentrations in the caption to the figures containing the chaperone activity are 3–6 orders of magnitude off: 213 μM MDH instead of 213 nM in the caption to Fig. 2 in Appia-Ayme et al. and 392 mM MDH instead of 392 nM in the caption to fig. 7 in Petit-Hartlein et al. [6,8]

A more informative chaperone activity measurement was performed by Appia-Ayme et al., which was based on the refolding of unfolded MDH in the presence of ZraP and to use MDH activity as a reporter of properly folded protein. In their case addition of a tenfold excess of ZraP in the presence of a large excess of Zn^{2+} was required to recover 10% of the MDH activity. According to these authors ZraP treated with EDTA was not able to protect folded MDH against denaturation. Addition of Zn in a ratio of 5–50 Zn^{2+} per ZraP monomer was required for chaperone activity. For chaperone assisted folding of MDH using GroEL/GroES the recovery is usually between 40 and 60% [30]. It has remained unclear how this chaperone like activity reported for ZraP compares to known chaperones like GroEL/ES or HSP40/70. Perhaps the effects observed for ZraP merely representing unspecific transient interactions with particular charged or hydrophobic domains.

Clearly expression of ZraP in *E. coli* is zinc responsive. However, the protein has no direct role in zinc tolerance. The fact that *E. coli* becomes more tolerant to high zinc concentrations after deletion of zraP favourably excludes the previously proposed zinc storage function, and is also in conflict with a putative chaperone function under zinc stress conditions. Apparently, *E. coli* produces ZraP under zinc stress conditions for a different reason. Finally, it may be possible that Zn^{2+} is not the primary target for ZraP. Perhaps ZraP has a role in the homeostasis of Cu or other metals.

4. Conclusions

We can conclude that ZraP is a Zn^{2+} and Cu^{2+} binding homo-octameric protein that has no direct role in zinc tolerance in *E. coli*. Despite this work and earlier research efforts the biological function of ZraP remains elusive. In order to solve this it would be very interesting to perform metalloproteomics experiments to characterize the response of *E. coli* to the *zraP* deletion in the presence of high zinc levels.

Conflicts of interest

Dr. Hagedoorn and Hagen report grants from The Netherlands Organisation for Scientific Research, NWO, during the conduct of the study.

Acknowledgements

Martijn Pinkse and Mervin Pieterse are acknowledged for performing the protein MS measurements on the purified ZraP protein. This research was supported by grant NWO–CW 700.55.004 from the Council for Chemical Sciences of The Netherlands Organisation for Scientific Research.

Abbreviations

BLAST	basic local alignment search tool
CFE	cell free extract
CV	column volume
GFP	Green fluorescent protein
HR ICP-MS	high resolution inductively coupled plasma mass spectrometry
ITC	Isothermal Titration Calorimetry
MDH	malate dehydrogenase
MIRAGE	Metal Isotope native RadioAutography in Gel Electrophoresis
OmpC	Outer membrane protein C
PMTR	*Proteus mirabilis* transcriptional regulator
TCEP	tris(2-carboxyethyl)phosphine
ZraP	zinc resistance associated protein
ZraSR	Two-component regulatory system consisting of a membrane associated sensor kinase ZraS and a cytoplasmic response regulator ZraR

Appendix A. Supplementary data

Supplementary data to this article can be found online at https://doi.org/10.1016/j.jinorgbio.2018.12.013.

References

[1] C.E. Outten, T.V. O'Halloran, Science 292 (2001) 2488–2492.
[2] L.J. Lee, J.A. Barrett, R.K. Poole, J. Bacteriol. 187 (2005) 1124–1134.
[3] J.A. Easton, P. Thompson, M.W. Crowder, J. Biomol. Tech. 17 (2006) 303–307.
[4] M. Noll, K. Petrukhin, S. Lutsenko, J. Biol. Chem. 273 (1998) 21393–21401.
[5] A.M. Sevcenco, M.W.H. Pinkse, H.T. Wolterbeek, P.D.E.M. Verhaert, W.R. Hagen, P.L. Hagedoorn, Metallomics 3 (2011) 1324–1330.
[6] C. Appia-Ayme, A. Hall, E. Patrick, S. Rajadurai, T.A. Clarke, G. Rowley, Biochem. J. 442 (2012) 85–93.
[7] S. Leonhartsberger, A. Huber, F. Lottspeich, A. Böck, J. Mol. Biol. 307 (2001) 93–105.
[8] I. Petit-Hartlein, K. Rome, E. de Rosny, F. Molton, C. Duboc, E. Gueguen,

A. Rodrigue, J. Coves, Biochem. J. 472 (2015) 205–216.
[9] M.T. Gomez-Sagasti, J.M. Becerril, I. Martin, L. Epelde, C. Garbisu, Cell Biol. Toxicol. 30 (2014) 207–232.
[10] A. Jaroslawiecka, Z. Piotrowska-Seget, Microbiology 160 (2014) 12–25.
[11] M.K. Maruthamuthu, I. Ganesh, S. Ravikumar, S.H. Hong, Biotechnol. Lett. 37 (2015) 659–664.
[12] S. Ravikumar, I.K. Yoo, S.Y. Lee, S.H. Hong, Bioprocess Biosyst. Eng. 34 (2011) 1119–1126.
[13] M. Sokołowska, W. Bal, J. Inorg. Biochem. 99 (2005) 1653–1660.
[14] F. Sievers, A. Wilm, D. Dineen, T.J. Gibson, K. Karplus, W. Li, R. Lopez, H. McWilliam, M. Remmert, J. Söding, J.D. Thompson, D.G. Higgins, Mol. Syst. Biol. 7 (2011).
[15] M.A. Larkin, G. Blackshields, N.P. Brown, R. Chenna, P.A. McGettigan, H. McWilliam, F. Valentin, I.M. Wallace, A. Wilm, R. Lopez, J.D. Thompson, T.J. Gibson, D.G. Higgins, Bioinformatics 23 (2007) 2947–2948.
[16] P. Dalgaard, T. Ross, L. Kamperman, K. Neumeyer, T.A. McMeekin, Int. J. Food Microbiol. 23 (1994) 391–404.
[17] T.L. Raivio, Biochim. Biophys. Acta 1843 (2014) 1529–1541.
[18] P.-L. Hagedoorn, L. van der Weel, W.R. Hagen, J. Vis. Exp. 93 (2014) e51611.
[19] J. Balk, A.J. Pierik, D.J. Netz, U. Muhlenhoff, R. Lill, EMBO J. 23 (2004) 2105–2115.
[20] U. Skoging, P. Liljeström, J. Mol. Biol. 279 (1998) 865–872.
[21] D.T. Ta, L.E. Vickery, J. Biol. Chem. 267 (1992) 11120–11125.
[22] Z.M. Anwar, J. Chin. Chem. Soc. 52 (2005) 863–871.
[23] A.E. Martell, R.M. Smith, Critical Stability Constants, Plenum Press, 1974.
[24] C.F. Quinn, M.C. Carpenter, M.L. Croteau, D.E. Wilcox, A.L. Feig (Ed.), Meth. Enzymol. vol. 567, Academic Press, 2016, pp. 3–21.
[25] J. Nagaj, K. Stokowa-Sołtys, E. Kurowska, T. Frączyk, M. Jeżowska-Bojczuk, W. Bal, Inorg. Chem. 52 (2013) 13927–13933.
[26] A. Krężel, J. Wójcik, M. Maciejczyk, W. Bal, Chem. Commun. (2003) 704–705.
[27] M. Jeżowska-Bojczuk, P. Kaczmarek, W. Bal, K.S. Kasprzak, J. Inorg. Biochem. 98 (2004) 1770–1777.
[28] L. Alderighi, P. Gans, A. Ienco, D. Peters, A. Sabatini, A. Vacca, Coord. Chem. Rev. 184 (1999) 311–318.
[29] Y. Zhang, S. Akilesh, D.E. Wilcox, Inorg. Chem. 39 (2000) 3057–3064.
[30] M. Hayer-Hartl, C. Schneider (Ed.), Chaperonin Protocols, Springer New York, Totowa, NJ, 2000, pp. 127–132 vol..